



# Fatigue life evaluation of welded joints under multiaxial loading for different stress concepts using an extended Gough-Pollard criterion

N. M. Bauer<sup>1</sup> · J. Baumgartner<sup>1</sup> · M. Fass<sup>2</sup>

Received: 26 September 2023 / Accepted: 5 February 2024 / Published online: 17 April 2024  
© The Author(s) 2024

## Abstract

Fatigue life evaluation of welded joints under multiaxial loading usually refers to stresses normal to the weld and shear stresses. Stresses parallel to the weld are not considered in most experiments or the well-known Gough-Pollard criterion. Hence, the Gough-Pollard criterion has recently been extended to include all stress components at the weld surface. In this paper, both the original and, for the first time, the extended Gough-Pollard criterion are applied to different welded specimens under multiaxial loading that includes stresses parallel to the weld. As shown, the original criterion is insufficient to evaluate such stress states. This is because the calculated fatigue life becomes less conservative as the stresses parallel to the weld become more significant. The extended criterion, on the other hand, shows greatly improved accuracy while significantly reducing the likelihood of non-conservative results. In conclusion, the extended Gough-Pollard criterion can describe fatigue life under multiaxial loading better than the original version and provides reliable and conservative results for welded joints. The main findings are valid for the nominal, the hot spot, and the notch stress concept.

**Keywords** Fatigue strength assessment · Multiaxial loading · Welded joints · Gough-Pollard

## Abbreviations

|                              |   |
|------------------------------|---|
| $\alpha$                     | Inclination angle, °  |
| $\sigma$                     | Normal stress, MPa  |
| $\sigma_{1/2}$               | Principal stress, MPa   |
| $\sigma_{\perp}$             | Stress normal to weld, MPa                                    |
| $\sigma_{\parallel}$         | Stress parallel to weld, MPa                                  |
| $\tau$                       | Shear stress, MPa   |
| $\nu$                        | Poisson's ratio, -  |
| $\Delta\sigma_{\perp}$       | Stress range normal to weld, MPa                              |
| $\Delta\sigma_{\perp,R}$     | Fatigue resistance against stress range normal to weld, MPa   |
| $\Delta\sigma_{\parallel}$   | Stress range parallel to weld, MPa                            |
| $\Delta\sigma_{\parallel,R}$ | Fatigue resistance against stress range parallel to weld, MPa |

|                |  |
|----------------|--|
| $\Delta\tau$   | Shear stress range, MPa                            |
| $\Delta\tau_R$ | Fatigue resistance against shear stress range, MPa |
| $f_N$          | Fatigue life evaluation factor, -                  |
| $\bar{f}_N$    | Averaged fatigue life evaluation factor, -         |
| $f_{N,norm}$   | Normalized fatigue life evaluation factor, -       |
| $k_{\sigma}$   | Slope of the S-N curve for normal stress, -        |
| $k_{\tau}$     | Slope of the S-N curve for shear stress, -         |
| $k^*$          | Slope of the S-N curve after the knee point, -     |
| $r_{ref}$      | Fictitious notch radius, mm                        |
| $t$            | Specimen thickness, mm                             |
| $t_f$          | Weld thickness at the location of failure, mm      |
| $w$            | Plate width, mm                                    |
| $CV$           | Comparison value, -                                |
| $CV_{\sigma}$  | Share of comparison value due to normal stress, -  |
| $CV_{\tau}$    | Share of comparison value due to shear stress, -   |
| $F$            | Force, N   |
| $K_s$          | Hot spot stress concentration factor, -            |
| $K_t$          | Notch stress concentration factor, -               |
| $N$            | Cycle number, -                                    |
| $N_{exp}$      | Experimental cycle number, -                       |
| $N_k$          | Cycle number at the knee point, -                  |
| $N_{num}$      | Numerically evaluated cycle number, -              |
| $R$            | Stress ratio, -                                    |

Recommended for publication by Commission XIII - Fatigue of Welded Components and Structures

✉ N. M. Bauer  
niklas.michael.bauer@lbf.fraunhofer.de

<sup>1</sup> Fraunhofer Institute for Structural Durability and System Reliability LBF, Darmstadt, Germany

<sup>2</sup> Mechanical Engineering Department, Research Group SAM, Technical University of Darmstadt, Darmstadt, Germany

## 1 Introduction

Many approaches in the literature and design codes deal with fatigue life evaluation of welded specimens subjected to multi-axial stress. Multi-axial stress usually refers to stress normal to the weld ( $\sigma_{\perp}$ ) and shear stress ( $\tau$ ) at the weld surface. Stresses parallel to the weld ( $\sigma_{\parallel}$ ) are usually not taken into consideration within experiments and various fatigue life evaluation approaches. One of these approaches is the well-known Gough-Pollard (GP) criterion as described in the IIW recommendations of 2016 [1]. The GP criterion originates from the work by Gough and Pollard [2] where an elliptical relationship between applied normal and shear stress for a given experimental fatigue life was shown for unwelded specimens. Since then, the GP criterion has been successfully applied to many different welded joints [3]. However, only very few studies used the same on welded specimens subjected to  $\sigma_{\parallel}$  [4, 5]. The application of  $\sigma_{\parallel}$  to specimens is expected to further contribute to the damage, thus increasing the likelihood of non-conservative estimates. Therefore, an extension of the GP criterion that includes all three stress components in the plane stress state has recently attracted attention. The extended Gough-Pollard criterion (EGP) has been proposed by DVS [6] and is included in the upcoming IIW recommendations [7]. To the knowledge of the authors, no comparative study or application of the EGP criterion on welded specimens has been conducted yet. Moreover, there is very little experimental data on welded specimens subjected to multi-axial loading including  $\sigma_{\parallel}$  in the literature. The aim of this paper is the application and validation of the EGP criterion as well as the comparison with the GP criterion based on available experimental data. While the formulation of the EGP criterion in [6] has been proposed for the notch stress concept, this paper examines the EGP criterion within the nominal, the hot spot, and the notch stress concept individually.

## 2 Fatigue life assessment approaches

For fatigue assessment of welded joints under multi-axial loading the IIW recommendations from 2016 [1] suggest the use of the well-known GP criterion

$$\left(\frac{\Delta\sigma_{\perp}}{\Delta\sigma_{\perp,R}(N)}\right)^2 + \left(\frac{\Delta\tau}{\Delta\tau_R(N)}\right)^2 \leq CV \quad (1)$$

where  $\Delta\sigma_{\perp}$  denotes the acting stress range normal to the weld and  $\Delta\tau$  the acting shear stress range. The normal stress  $\sigma$  has been substituted by the stress normal to the weld  $\sigma_{\perp}$  in accordance with the usual understanding and all applications of the GP criterion known to the authors.  $\Delta\sigma_{\perp,R}(N)$  and  $\Delta\tau_R(N)$  represent the fatigue resistance at a given number of cycles  $N$  based on the respective design S-N curve for

uniaxial loading. Depending on whether the type of loading is proportional or non-proportional the comparison value  $CV$  takes values of 1 or 0.5. A load is non-proportional when the ratio between two different types of stress is not constant, implying a change in the direction of the principal stress. Reducing the comparison value from 1 to 0.5 results in a lower predicted fatigue life. The reasoning behind this is that non-proportional stress states applied to ductile materials result in lower fatigue life compared to proportional stress states [8]. The fatigue life can be calculated by numerically solving equation (1) with respect to  $N$ . In accordance with the available data, only constant loading was considered. Figure 1 illustrates the relationship between the two stress components for given cycle numbers  $N_1$  and  $N_2$ . The index  $R$  denotes the endurable stresses, i.e., the resistance, for uniaxial loading at the corresponding cycle number.

To additionally consider  $\Delta\sigma_{\parallel}$ , the EGP criterion as formulated in [6] and [7] completes the original formulation as follows:

$$\left(\frac{\Delta\sigma_{\perp}}{\Delta\sigma_{\perp,R}(N)}\right)^2 + \left(\frac{\Delta\tau}{\Delta\tau_R(N)}\right)^2 + \left(\frac{\Delta\sigma_{\parallel}}{\Delta\sigma_{\parallel,R}(N)}\right)^2 \leq CV \quad (2)$$

with  $\Delta\sigma_{\parallel}$  as the applied stress range parallel to weld and  $\Delta\sigma_{\parallel,R}(N)$  as the fatigue design S-N curve for uniaxial stresses parallel to weld. Both approaches can be applied based on the nominal, the hot spot, or the notch stress concept. Only when the notch stress concept is used in combination with the EGP criterion,  $\sigma_{\parallel}$  determined in the notch cannot be used. The reason is that even under pure  $\sigma_{\perp}$ ,  $\sigma_{\parallel}$  is introduced as well. Under plain strain conditions and  $\sigma_{\perp}$  only, these stresses can be calculated by

$$\sigma_{\parallel} = \nu \cdot \sigma_{\perp} \quad (3)$$

with  $\nu$  being the Poisson's ratio. The Poisson effect describes how an applied force leads to deformations perpendicular to

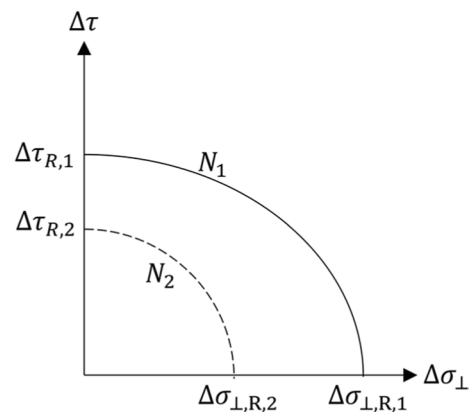


Fig. 1 Exemplary representation of the Gough-Pollard ellipsoid

the direction of the load. Due to the notch effect at the weld, a local stress concentration is observed when  $\sigma_{\perp}$  is applied. The higher deformation at the weld due to the Poisson effect is partially prevented as the stress concentration is only local and the remaining parts of the specimen are subjected to lower deformation. Thus, a local stress parallel to the weld acts implicitly. Evaluating  $\sigma_{\parallel}$  in the notch under multiaxial stress conditions is no longer feasible as it cannot always be distinguished whether the stress originates from an external force or from the obstruction of transverse contraction. However, any design S-N curve already takes such implicit stresses into account, so only externally introduced stresses must be evaluated. To overcome this issue, while still considering  $\sigma_{\parallel}$ , the term of the EGP criterion including  $\sigma_{\parallel}$  is not based on the notch stress but on the nominal stress and the respective fatigue resistance.

### 3 Methodology

The assessment of fatigue life in this paper is based on experimental data from the literature and projects. Both the GP and the EGP criterion were used to predict fatigue life based on the nominal, the hot spot, and the notch stress concept. The following chapter provides an overview of the specimens and their characteristics, loading conditions, fatigue resistance for each specimen and stress component, and the approach used to evaluate and validate the EGP criterion.

#### 3.1 Experimental data

Four different types of specimens subjected to multiaxial stress states which include stresses parallel to the weld

were identified from the literature. Throughout this paper, all specimen types are referred to by their primary author including Bokesjö [4], Khurshid [5], Shen [9], and Takahashi [10]. The results of the recently completed project *LaserMultiAx* [11] were also considered. The specimen types included butt-welded flat specimens from Khurshid, LaserMultiAx, and Shen, and the fillet-welded cruciform joints from Bokesjö and Takahashi. All specimens were made of steel. As the specimens from Bokesjö, Khurshid, and LaserMultiAx were manufactured with different weld seam angles and the loading conditions for Shen and Takahashi differed, a total of 17 different test sets could be considered for fatigue life assessment. Figure 2 shows exemplary the types of specimens (the weld inclinations of the first three specimens are presented at an angle of 45°).

An overview of the fatigue tests and specimen types is given in Table 1. The specimens from Khurshid were ground flush on the surface while all other specimens remained in an as-welded condition. The specimens from Bokesjö and Khurshid were not welded through, resulting in a root gap, which was the location of failure. The specimens from LaserMultiAx and Shen were welded through and the specimens failed at the weld toe. For the specimens from Takahashi, failure was mainly observed at the short edge of the weld toe. The two fatigue tests where the crack initiated at the long edge of the weld and three specimens from Bokesjö which did not fail in the root were excluded in this paper. The failure criterion for all experiments from the literature was total fracture. The fatigue life of specimens from LaserMultiAx was defined as the number of cycles until the initiation of a technical crack.

The first three specimens were subjected to a uniaxial load  $F$  of constant amplitude in the longitudinal direction

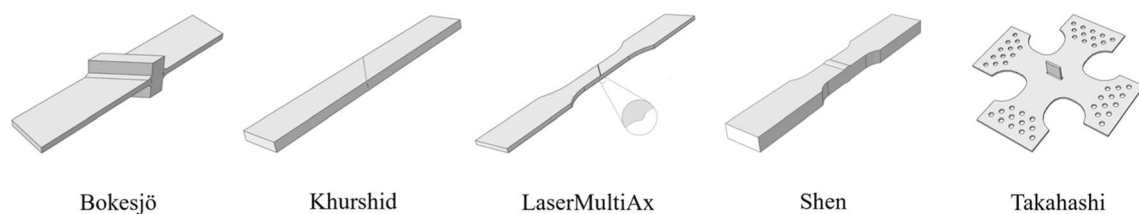


Fig. 2 Exemplary representation of all types of specimens

Table 1 Specimens and fatigue test characteristics

| Primary author    | Type      | Weld seam inclination    | Plate thickness in mm | R-values   | Failure location      | Failure criterion |
|-------------------|-----------|--------------------------|-----------------------|------------|-----------------------|-------------------|
| Bokesjö [4]       | Cruciform | 0°, 15°, 45°             | 16                    | 0.08 – 0.1 | Weld root             | Fracture          |
| Khurshid [5]      | Flat      | 0°, 45°, 60°, 70°        | 16.00 – 17.14         | 0.1        | Weld root             | Fracture          |
| LaserMultiAx [11] | Flat      | 0°, 22.5°, 45°, 60°, 90° | 4                     | 0          | Weld toe              | Crack initiation  |
| Shen [9]          | Flat      | 0°                       | 35                    | 0, -∞      | Weld toe              | Fracture          |
| Takahashi [10]    | Cruciform | 0°                       | 12                    | 0, -∞      | Weld toe (short edge) | Fracture          |

and manufactured with different weld seam angles  $\alpha$  ranging from  $0^\circ$  to  $90^\circ$ . For any weld seam inclination between  $0^\circ$  and  $90^\circ$ , a uniaxial load  $F$  leads to a multiaxial stress state, where each stress component of the plane stress state appears according to Fig. 3 and Fig. 4. Eqs. (4) to (6) show how each stress component is calculated with a plate width  $w$  and a weld thickness  $t_f$  at the failure location. The weld thickness is equal to the sum of both weld throat thicknesses in the case of partial penetration and equal to the specimen thickness  $t$  in the case of full penetration.

$$\sigma_{\perp} = \frac{F}{t_f \cdot w} \cos^2(\alpha) \tag{4}$$

$$\sigma_{\parallel} = \frac{F}{t_f \cdot w} \sin^2(\alpha) \tag{5}$$

$$\tau = \frac{F}{t_f \cdot w} \sin(\alpha) \cos(\alpha) \tag{6}$$

The specimens of Shen were fabricated without any weld seam inclination, but the weld seam was subjected to a second constant amplitude pressure in the direction longitudinal to the weld, resulting in stresses parallel to the weld. The pressure was applied to the side of the specimen covering the weld and the immediate area around. The stresses normal to the weld resulted from bending. The specimens from Takahashi were subjected to constant amplitude loads in the direction longitudinal and transverse to the attachment, resulting in stresses normal and stresses parallel to the weld at the short edge. Unlike the first three specimens, where an applied load could only result in proportional stress states, the different stress components could be applied independently. This allowed non-proportional loading with a  $180^\circ$  phase shift between the two normal stresses to be applied to some of the specimens from Takahashi.

### 3.2 Stress concepts and FE modeling

A comprehensive comparison of the GP and the EGP approach is based on nominal stresses, hot spot stresses, and notch stresses individually. The nominal stresses at the failure location could be derived directly from the literature or had to be calculated from the applied forces and given geometry. For the specimens of Shen and Takahashi, the stresses at the weld were computed by Finite Element (FE)

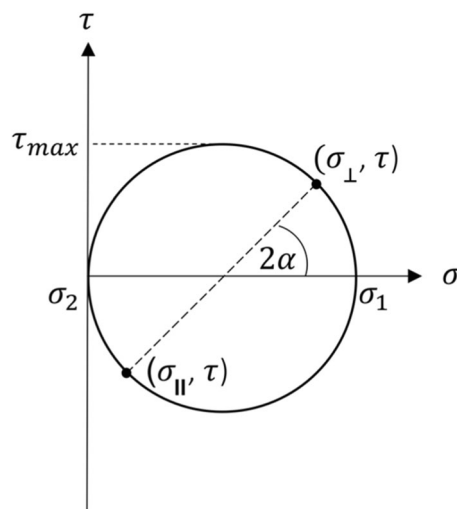


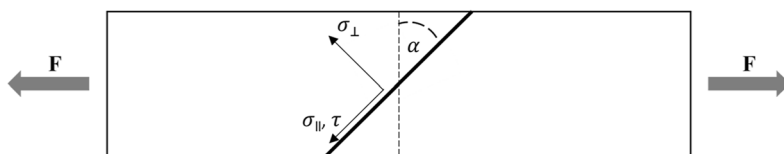
Fig. 4 Mohr's circle for flat specimens with a weld inclination  $\alpha$

simulation, neglecting the welded attachment. To derive the structural hot spot stress and the notch stress at the failure location, FE models based on 3D-solid hexahedral elements with a quadratic shape function were created for each specimen type. The hot spot stress for each stress component was derived by linear extrapolation toward the weld from the reference points at a  $0.4t$  and  $1t$  distance normal to the weld according to IIW type “a” hot spots [7]. Only for the specimens from Bokesjö and Khurshid, the hot spot stress was not derived as the specimens contained root gaps at the weld for which the hot spot stress is not defined. The notch stress was derived in a similar way, with the notch area meshed according to [12] with an error of 2% or less. The fictitious notch radius for modeling was chosen based on the plate thickness with  $r_{ref} = 1\text{mm}$  for plates with  $t \geq 5\text{mm}$  and  $r_{ref} = 0.05\text{mm}$  otherwise according to [7]. The root gaps are modeled with a thickness of 0.1 mm. A stress concentration factor (SCF), defined as the hot spot respectively the notch stress divided by the nominal stress, is derived for each relevant stress component of each specimen, and given in Table 2.

### 3.3 Fatigue life evaluation

The fatigue life prediction of both approaches depends on the applied stresses as well as the design S-N curves for

Fig. 3 Multiaxial stress state of flat specimens subjected to uniaxial loading



each stress component. As shown in Fig. 4, it is not possible to apply shear stress to most of the specimens in this paper without applying normal stresses simultaneously. Only the specimens from LaserMultiAx were subjected to  $\sigma_{\parallel}$  only. Therefore, the design S-N curves could not be directly derived from experimental data but were selected based on the corresponding FAT classes from the IIW recommendations [7]. Since the purpose of these S-N curves is to ensure a safe design of welds, all design S-N curves represent a survival probability of 97.7% and are defined for higher mean stresses with R-ratios of  $R = 0.5$ . The fatigue life prediction is therefore usually conservative. The FAT classes of the design S-N curves for nominal, hot spot, and notch stresses derived from the IIW recommendations are presented in Table 3. Within the hot spot stress concept, the FAT classes for  $\tau$  and  $\sigma_{\parallel}$  were chosen equal to those for the nominal stress. The FAT classes for the notch stress concept were differentiated according to the fictitious notch radius assumed in the FE models. According to the IIW recommendations, the FAT classes must be adjusted if certain conditions are met. All FAT classes within the nominal or the hot

spot (type “a”) stress concept refer to plate thicknesses of up to 25 mm. Since the specimens from Shen had a thickness of 35 mm, a thickness correction had to be applied for nominal and hot spot stresses. For butt joints, a thickness correction exponent of 0.2 gives a thickness reduction factor of 0.93. All R-ratios differed from  $R = 0.5$ . As there is no evidence of lower residual stresses and all R-ratios were consistently close to zero, no mean stress correction was applied. Adjustments to the FAT classes due to the remaining influencing factors, such as improvement techniques, are not relevant.

Following the IIW recommendations, slope values of  $k_{\sigma} = 3$  and  $k_{\tau} = 5$  were assumed for thick plates with  $t \geq 7\text{mm}$ . For thin plates with  $t < 7\text{mm}$ ,  $k_{\sigma} = 5$  and  $k_{\tau} = 7$  were used. The knee point was set to  $N_k = 10^7$  for normal and  $N_k = 10^8$  for shear stresses and the slope after the knee point was set to  $k^* = 22$ . The fatigue life  $N$  of each fatigue test was numerically calculated using both the GP and the EGP criterion. A fatigue life evaluation factor  $f_N$  was then derived as follows:

$$f_N = \frac{N_{num}}{N_{exp}} \tag{7}$$

**Table 2** Stress concentration factors for hot spot and notch stresses – The notch SCF are based either on a fictitious reference radius of 1 mm (no marking) or 0.05 mm (\*)

| Specimen           | Hot spot SCF $K_s$ |        |                      | Notch SCF $K_t$  |        |
|--------------------|--------------------|--------|----------------------|------------------|--------|
|                    | $\sigma_{\perp}$   | $\tau$ | $\sigma_{\parallel}$ | $\sigma_{\perp}$ | $\tau$ |
| Bokesjö 0°         | -                  | -      | -                    | 5.12             | -      |
| Bokesjö 15°        | -                  | -      | -                    | 5.10             | 3.32   |
| Bokesjö 45°        | -                  | -      | -                    | 6.42             | 2.88   |
| Khurshid 0°        | -                  | -      | -                    | 6.94             | -      |
| Khurshid 45°       | -                  | -      | -                    | 6.87             | 4.65   |
| Khurshid 60°       | -                  | -      | -                    | 6.52             | 4.26   |
| Khurshid 70°       | -                  | -      | -                    | 9.15             | 4.67   |
| LaserMultiAx 0°    | 1.06               | -      | -                    | 2.60*            | -      |
| LaserMultiAx 22.5° | 1.01               | 1.01   | 1.00                 | 2.70*            | 2.15*  |
| LaserMultiAx 45°   | 1.02               | 1.02   | 1.01                 | 3.08*            | 2.13*  |
| LaserMultiAx 60°   | 1.01               | 1.01   | 1.00                 | 4.02*            | 2.14*  |
| LaserMultiAx 90°   | -                  | -      | 1.00                 | -                | -      |
| Shen               | 1.06               | -      | 1.02                 | 2.12             | -      |
| Takahashi          | 1.35               | -      | 0.94                 | 3.32             | -      |

To evaluate and compare the quality of the two approaches, averaged factors  $\overline{f_N}$  were calculated for each criterion and each test set separately. A test set in this context refers to a specific type of load applied to the same specimen configuration (e.g., with the same weld inclination). Since the design S-N curves do not represent the exact fatigue resistance of the specimens considered in this paper, i.e., the S-N curve with a 50% survival probability, all specimen types were evaluated based on different levels of conservatism, which can be interpreted as different safety factors. In the following, the term safety factor is used only to refer to this level of conservatism. Comparing the  $\overline{f_N}$  of different specimen types, which are based on different safety factors, requires some form of normalization. This was done by dividing all  $\overline{f_N}$  by the  $\overline{f_N}$  of the respective uniaxial test sets as they were not influenced by any multiaxial stress hypothesis and represent the predetermined safety factor, resulting from the selected FAT class. Since  $\sigma_{\perp}$  was the only stress component that all specimen types experienced alone, the corresponding test sets were selected for normalization. Accordingly, a fatigue life hypothesis, that correctly evaluates

**Table 3** FAT classes based on the IIW recommendations for nominal, hot spot, and notch stresses – FAT classes for notch stresses are based either on a fictitious notch radius of 1 mm (no marking) or 0.05 mm (marked with \*)

| Specimen type | FAT classes          |              |                          |                     |             |                         |                        |                |
|---------------|----------------------|--------------|--------------------------|---------------------|-------------|-------------------------|------------------------|----------------|
|               | $\sigma_{\perp,nom}$ | $\tau_{nom}$ | $\sigma_{\parallel,nom}$ | $\sigma_{\perp,hs}$ | $\tau_{hs}$ | $\sigma_{\parallel,hs}$ | $\sigma_{\perp,notch}$ | $\tau_{notch}$ |
| Bokesjö       | 63                   | 80           | 112                      | -                   | -           | -                       | 225                    | 160            |
| Khurshid      | 36                   | 80           | 112                      | -                   | -           | -                       | 225                    | 160            |
| LaserMultiAx  | 90                   | 100          | 125                      | 100                 | 100         | 125                     | 500*                   | 240*           |
| Shen          | 84                   | -            | 104                      | 93                  | -           | 104                     | 225                    | 160            |
| Takahashi     | 71                   | -            | 112                      | 100                 | -           | 112                     | 225                    | 160            |

multiaxial stress states, should show the same  $\overline{f_N}$  as for uniaxial loading. However, that applies only under the condition that all design S-N curves are similarly conservative. Finally, the averaged and normalized fatigue life prediction factor  $f_{N,norm,i}$  of one test set  $i$ , was calculated according to:

$$f_{N,norm,i} = \frac{\overline{f_{N,i}}}{\overline{f_{N,\sigma_{\perp}}}} \quad (8)$$

where  $\overline{f_{N,\sigma_{\perp}}}$  denotes the averaged fatigue life evaluation factor of the test set of the same specimen type subjected to only  $\sigma_{\perp}$ .  $\sigma_{\parallel}$  is not considered within the GP criterion. Any deviation in terms of  $f_{N,norm} > 1$  indicates a missing consideration of  $\sigma_{\parallel}$ . Applying the EGP criterion to the same data is expected to show  $f_{N,norm} \approx 1$  in order to prove the EGP criterion successful.  $f_{N,norm}$  will be referred to as normalized fatigue life factor (NFF).

To better understand if and when a certain stress component has a significantly damaging effect and when the EGP criterion is beneficial to the GP criterion, the influence of each stress component on fatigue life, in particular of  $\sigma_{\parallel}$ , must be quantified. Since the analyzed criteria consider the specific damage of each stress component individually (see Equations (1) and (2)), the contribution of each stress component to the calculated total damage can be assessed based on the corresponding share of the comparison value. The calculated total damage is inherently equal to the comparison value  $CV$  for any cycle number  $N$ . The calculated damage contribution from an exemplary stress component  $\sigma$  was derived as follows:

$$CV_{\sigma} = \frac{\left(\frac{\Delta\sigma}{\Delta\sigma_R(N)}\right)^2}{CV} \quad (9)$$

This provides the opportunity to confirm how the consideration of  $\sigma_{\parallel}$  significantly contributes to a better assessment of fatigue life. Knowing which stress component is primarily responsible for the failure according to the calculations further allows a comparison with the actual crack propagation type and the corresponding dominant stress component. Thus, a statement can be made as to whether the EGP criterion correctly identifies and evaluates the dominant stress components based on the chosen design S-N curves.

#### 4 Evaluation of the Gough-Pollard and extended Gough-Pollard criterion

The results of the fatigue life assessment are presented for each stress concept separately. For better interpretation and comparison of the results, the normalized fatigue data and design S-N curves are shown in Appendix 1. Normalized in this context means that all applied and endurable

stresses were divided by their respective FAT classes. All data refer to uniaxial stress states. Finally, the calculated damage contributions of each stress component were derived, analyzed, and compared to the actual crack initiation and propagation types of each test set.

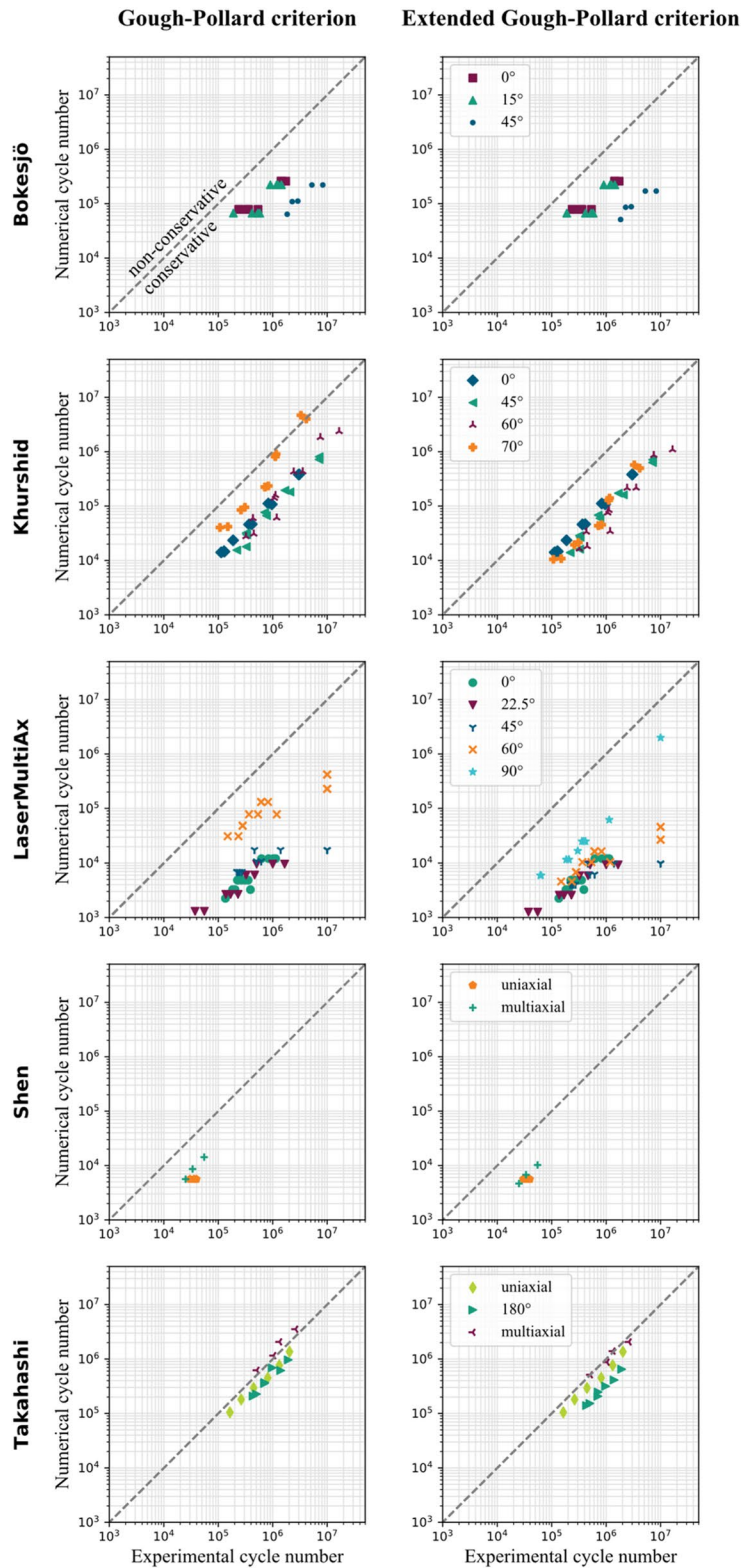
#### 4.1 Fatigue life evaluation

In the following section, the numerically calculated fatigue life based on the nominal stress concept is presented and compared with the experimental fatigue life in the form of N-N plots and the corresponding NFF. Figure 5 shows a separate N-N plot for each specimen type and assessment approach.

The dashed lines in the N-N plots of Fig. 5 represent a fatigue life prediction factor of  $f_N = 1$ . Any parallel shift of this line represents a specific  $f_N$ . An approach can be considered successful when all test sets are on the same line and exhibit a similar  $f_N$ . This means that all tests are evaluated with a similar level of conservatism, regardless of the specific stress state. The requirement to observe such behavior is that all design S-N curves are similarly conservative. When a stress component becomes more dominant in terms of applied stress relative to endurable stress, the prediction tends to align with the level of conservatism implied by the fatigue resistance of that stress component. Hence, if the S-N curves are of different conservativeness, there is a scatter introduced, which is not a result of the chosen approach. However, in the nominal stress concept, this requirement appears to be largely met. If all S-N curves have the same level of conservatism and the results still appear to be dependent on the stress state, this means that the approach is not suitable to correctly describe fatigue life. In conclusion, the evaluation approach correctly describes fatigue life if the same  $\overline{f_N}$  can be derived for different stress states.

Figure 5 shows on the left that evaluating only  $\sigma_{\perp}$  and  $\tau$  is insufficient, as increasing  $\sigma_{\parallel}$  leads to less conservative results. While most of the evaluations are close to each other, some specimens subjected to higher  $\sigma_{\parallel}$  exhibit significant deviations. The height and proportion of  $\sigma_{\parallel}$  increase simultaneously with an increasing weld inclination (see Equation (5)), respectively, for all test set–labeled multiaxial.  $\sigma_{\perp}$  and  $\tau$  can be ruled out as reasons for less conservative results since the 45° inclined specimens, which experienced the highest (proportion of)  $\tau$  (see Fig. 4), show similarly conservative results to the specimens subjected to  $\sigma_{\perp}$  alone. In addition, the specimens from Shen and Takahashi show the same behavior without experiencing any  $\tau$ . Some cases with higher  $\sigma_{\parallel}$  even show non-conservative evaluations despite the high survival probability of the design S-N curves. The 45° inclined

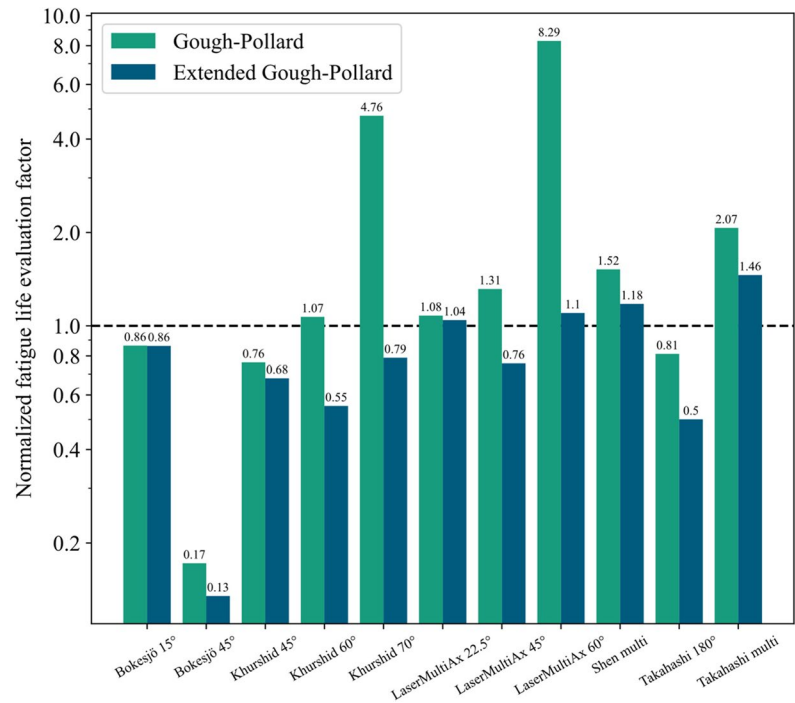
**Fig. 5** Numerically evaluated fatigue life over experimental fatigue life based on the nominal stress concept



test set from Bokesjö shows unusual behavior because this test set showed higher fatigue life at lower loads than the other two test sets. The specimens from LaserMultiAx with a weld inclination of 90° are not displayed for the GP

criterion because a 90° inclination implies that  $\sigma_{\parallel}$  is the only applied stress component and  $\sigma_{\parallel}$  cannot be evaluated. On the right, Fig. 5 shows how the EGP criterion consistently reduces the predicted fatigue life compared to the GP

**Fig. 6** Normalized fatigue life evaluation factor for each multiaxial test set based on the nominal stress concept



criterion. This is because the term including  $\sigma_{\parallel}$  in Equation (2) can be interpreted as additional damage. All evaluations exhibit a similar  $\overline{f}_N$ , thus significantly reducing the scatter and increasing the prediction accuracy. In addition, there are no non-conservative results after evaluation by the EGP criterion anymore. The results for LaserMultiAx exhibit different levels of conservatism for the two uniaxially stressed test sets. Assuming that the 90° inclined specimens had the same safety factor as the 0° inclined specimens, all results would move even closer together.

To better understand whether the EGP criterion correctly evaluates the multiaxial stress state including the damaging effect of  $\sigma_{\parallel}$ , the NFF (see Equation (8)) can provide more precise information. The results for the NFF regarding each test set based on the nominal stress concept are presented in Fig. 6. A NFF of one represents an optimal prediction as there is no difference between predicting the life under uniaxial or multiaxial stresses and the calculated fatigue life is equal to the experimental fatigue life with a certain safety factor. A theoretical factor of  $\infty$  represents the worst case for the GP criterion, where only  $\sigma_{\parallel}$  is significant and the other stress components approximate zero.

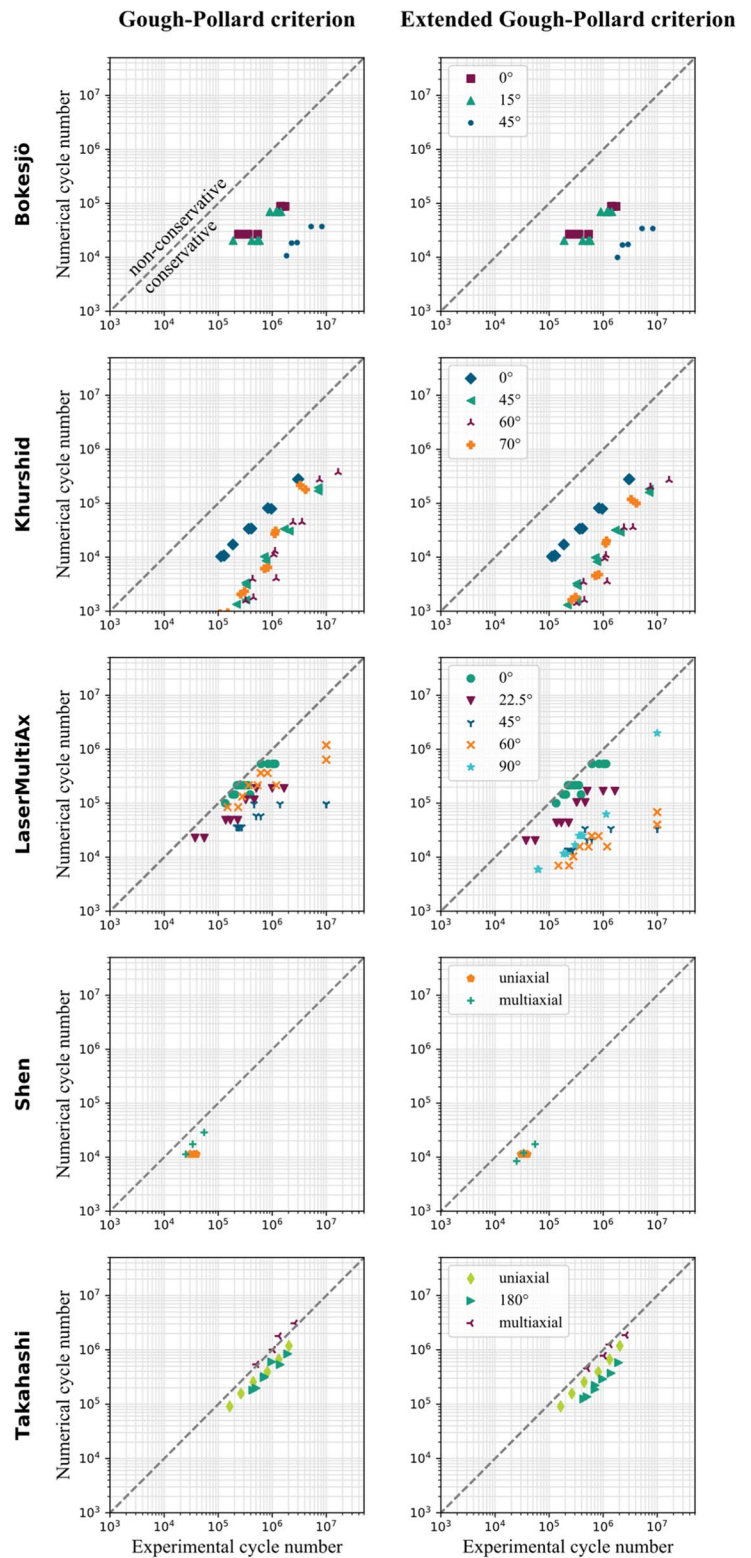
Figure 6 shows the NFF of all test sets on a logarithmic scale. The logarithmic scale ensures a consistent presentation of the results and reflects the distance in the logarithmic N-N plots. Any NFF greater than one represents less conservative results and should be avoided. Specimens subjected to higher  $\sigma_{\parallel}$  cannot be correctly evaluated by the GP criterion as  $f_{N,norm} > 1$  for most cases. In particular, the 70° inclined test set from Khurshid and the 60° inclined test set from LaserMultiAx show high deviations with a NFF of

up to 8.29. This means that the calculated fatigue life for the respective test set under multiaxial loading is on average 8.29 times higher than the calculated fatigue life for the 0° inclined specimens. The EGP criterion gives significantly better results than the GP criterion as a much smaller deviation from  $f_{N,norm} = 1$  is shown over all the different specimens and loads. For the specimens considered, the EGP criterion can reduce the maximum NFF from 8.29 to 1.46. All the major deviations resulting from the GP criterion are corrected when the EGP criterion is used, and the prediction accuracy is significantly improved by reducing the scatter between different test sets. The test set from Bokesjö at a 45° angle is ignored in the following considerations due to the aforementioned reason. The test set from Takahashi is assessed based on a comparison value of  $CV = 0.5$  (see Eqs. (1) and (2)) to compensate for the reduced fatigue life due to non-proportional loading. Thus, the evaluation is already very conservative and the test set is also neglected further on. For the remaining test sets, the minimum NFF decreases from 0.76 to 0.55. Lower NFF are generally not critical for the safe design of welds as they are more conservative. A more conservative evaluation of  $\tau$  compared to  $\sigma_{\perp}$  explains why some NFF are already close to or below one when using the GP criterion alone, leading to slightly worse results when using the EGP criterion as the NFF decreases further.

The results of both approaches within the hot spot stress concept tend to be similar to those within the nominal stress concept. Therefore, the main findings are similar. Due to the root gap in many specimens, for which the hot spot stress is not defined, not all specimens can be evaluated. The similarity of



**Fig. 7** Numerically evaluated fatigue life over experimental fatigue life based on the notch stress concept



the results of the remaining specimens can be explained by a SCF close to one and little difference between the FAT classes of the nominal and the hot spot stress concept. All results are shown in Appendix 1 and 2 for a more detailed inspection.

The notch stress concept shows partially different results from the other two stress concepts. Figure 7 shows a separate N-N plot for each assessment criterion and each specimen type within the notch stress concept. Again, for a better

understanding of all the diagrams, the normalized fatigue data is added to Appendix 1 with the corresponding design S-N curve.

The N-N plots for specimens from Shen and Takahashi in Fig. 7 remain similar to those based on nominal or hot spot stresses. All specimens from Khurshid subjected to  $\tau$  are evaluated significantly more conservative than those subjected only to  $\sigma_{\perp}$ . Apparently, the higher  $\tau$ , which peaks at an inclination of  $45^{\circ}$ , the lower the calculated fatigue life. This indicates that the FAT class for  $\tau$  is much more conservative than that for  $\sigma_{\perp}$ , which will later be analyzed in detail. Adding  $\sigma_{\parallel}$  to the evaluation further reduces the calculated fatigue life. The N-N plot for the project LaserMultiAx also shows how the two uniaxially loaded test sets are evaluated differently conservatively (see Appendix 1). Adding shear stress considerably increases the conservatism. Accordingly, there occurs a deviation between all test sets, making predictions inaccurate. Figure 8 illustrates the NFF of both criteria for the notch stress concept.

### 4.2 Damage contribution and types of crack propagation

In order to better understand the effect of every stress component on fatigue life, a detailed inspection of all stress components and their contribution to the overall damage, as evaluated based on the EGP criterion (see Eq. (9)), is advantageous. Additionally, a comparison was conducted with the actual failure types of each specimen to further assess whether the EGP criterion correctly describes the most damaging stress component. Four different failure types in terms of crack initiation and propagation were observed and are exemplarily illustrated for a part of the weld in Fig. 9. The crack always initiates in the weld and propagates either along the weld or in the base material perpendicular to the applied load.

The four failure types can now be assigned to their corresponding stress component. The stress component  $\sigma_{\perp}$  leads to crack initiation and propagation perpendicular to  $\sigma_{\perp}$  and along the weld (type 2). Similarly,  $\sigma_{\parallel}$  results in

**Fig. 8** Normalized fatigue life evaluation factor for each multi-axial test set based on the notch stress concept

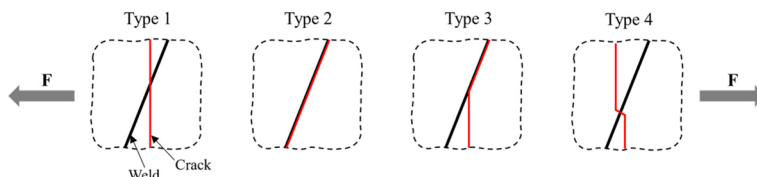
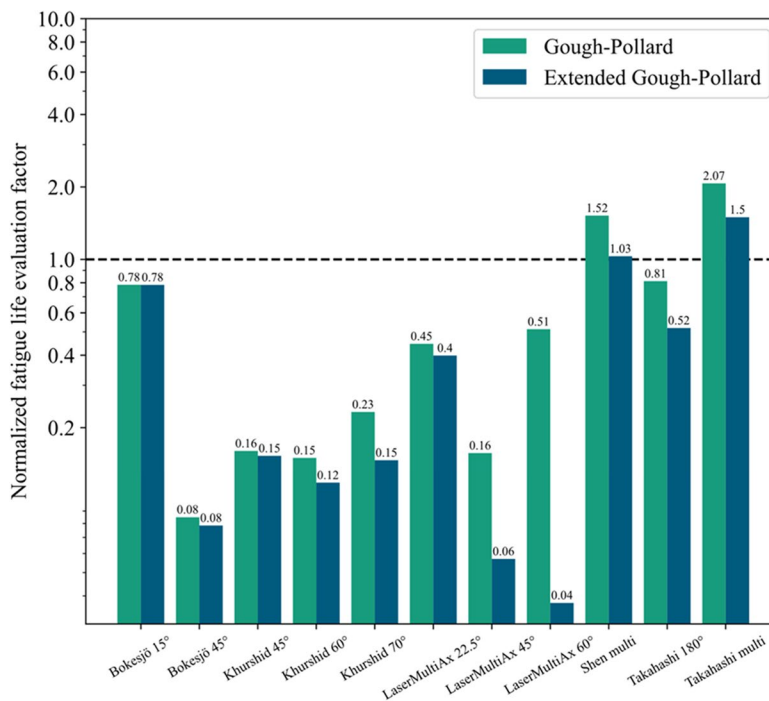


**Fig. 9** Types of crack propagation at the weld—type 1: crack propagation normal to the load, type 2: crack propagation along the weld, type 3: combination of type 1 and type 2, type 4: crack propagation normal to the weld

crack initiation perpendicular to both  $\sigma_{\parallel}$  and the weld, but propagation perpendicular to the load once the crack reaches the base material (type 4). When  $\tau$  is the dominant stress component, the crack initiates at an angle of  $45^\circ$  to the weld. Hence, the crack initiates and propagates perpendicular to the load given a weld inclination of  $45^\circ$ . Weld inclinations that are not too far from  $45^\circ$  result in similar cracks as the crack quickly reaches the base material (type 1). If both  $\sigma_{\perp}$  and  $\tau$  are similarly damaging, a combination of type 1 and type 2 can occur (type 3). For the extreme scenarios of  $0^\circ$  or  $90^\circ$ , failure type 1 equals type 2 respectively type 4. Table 4 summarizes the dominant failure type for each test set as well as the contribution of each stress component to the overall damage (see Eq. (9)) in the form of a range, representing all fatigue tests in a test set for the nominal and notch stress concept. The hot spot stress concept proved to be similar to the nominal stress concept and is therefore not presented.

Assuming that the EGP criterion correctly evaluates the fatigue life under multiaxial loading,  $CV_{\sigma/\tau}$  represents the actual proportion of damage caused by a stress component. Table 4 explains how test sets with a higher damage contribution of  $\sigma_{\parallel}$  exhibit greater deviations when using only the GP criterion, and how the more accurate predictions of the EGP criterion are due to the consideration of the damaging effect of  $\sigma_{\parallel}$ . Since the effect of a stress component depends on the fatigue resistance of the same as well as the other stress components and their respective fatigue resistances, the importance of considering  $\sigma_{\parallel}$  cannot be estimated in

advance. Therefore, the EGP criterion must always be used. Table 4 further confirms that the FAT class for  $\tau$  within the notch stress concept is too low. The comparatively low FAT class dominates the assessment and increases the calculated damage as well as the importance of the same stress component. Consequently, all test sets from Khurshid are primarily evaluated based on  $\tau$  (with a  $CV_{\tau}$  of up to 90%).

The damage contributions provide insight into whether the EGP criterion correctly identifies the most damaging stress component. As expected, the previously described relationships between the dominant stress component and the corresponding failure type are confirmed for the most part. Those specimens from Khurshid with a  $70^\circ$  inclination are assigned to failure type 1 only. Whether the crack might have initiated perpendicular to the weld (type 4), as expected, has not been studied. However, type 1 comes close to type 4 for higher inclinations and distinguishing between type 1 and type 4 becomes more difficult. The specimens with an inclination of  $22.5^\circ$  from LaserMultiAx show failure according to type 1. Since the specimens from LaserMultiAx generally show little stress concentration at the notch due to the flat weld seam, the crack is less affected by the weld and quickly propagates in the base material perpendicular to the load. The failure type 4 for the specimens with a  $45^\circ$  weld inclination can only be partially explained, indicating that the chosen FAT classes might require adjustment for the given specimens. However, Table 4 further supports the hypothesis that the EGP criterion accurately evaluates the effect of all stress components on fatigue life.

**Table 4** Failure type and range of damage contribution of each stress component calculated from the EGP criterion for the nominal and the notch stress concept in %

| Test set                  | Failure types | Nominal stress concept |             |                           | Notch stress concept  |             |                           |
|---------------------------|---------------|------------------------|-------------|---------------------------|-----------------------|-------------|---------------------------|
|                           |               | $CV_{\sigma_{\perp}}$  | $CV_{\tau}$ | $CV_{\sigma_{\parallel}}$ | $CV_{\sigma_{\perp}}$ | $CV_{\tau}$ | $CV_{\sigma_{\parallel}}$ |
| Bokesjö $0^\circ$         | 2             | 100                    | 0           | 0                         | 100                   | 0           | 0                         |
| Bokesjö $15^\circ$        | 2             | 90 – 92                | 8 – 10      | 0                         | 83 – 87               | 13 – 17     | 0                         |
| Bokesjö $45^\circ$        | 3,2           | 34 – 40                | 47 – 55     | 11 – 13                   | 37 – 44               | 51 – 60     | 4                         |
| Khurshid $0^\circ$        | 2             | 100                    | 0           | 0                         | 100                   | 0           | 0                         |
| Khurshid $45^\circ$       | 2             | 54 – 73                | 19 – 41     | 6 – 8                     | 13 – 36               | 61 – 85     | 1 – 3                     |
| Khurshid $60^\circ$       | 1,3           | 24 – 38                | 27 – 53     | 23 – 35                   | 5 – 16                | 70 – 90     | 4 – 14                    |
| Khurshid $70^\circ$       | 1             | 8 – 11                 | 24 – 47     | 45 – 65                   | 3 – 8                 | 69 – 89     | 8 – 23                    |
| LaserMultiAx $0^\circ$    | 2             | 100                    | 0           | 0                         | 100                   | 0           | 0                         |
| LaserMultiAx $22.5^\circ$ | 1             | 75 – 79                | 20 – 24     | 1                         | 54 – 59               | 37 – 42     | 4                         |
| LaserMultiAx $45^\circ$   | 1,4           | 32 – 33                | 49 – 52     | 16 – 17                   | 16 – 17               | 55 – 58     | 26 – 28                   |
| LaserMultiAx $60^\circ$   | 4             | 10 – 11                | 39 – 46     | 45 – 50                   | 6 – 7                 | 35 – 41     | 53 – 58                   |
| LaserMultiAx $90^\circ$   | 4             | 0                      | 0           | 100                       | 0                     | 0           | 100                       |
| Shen uniaxial             | 2             | 100                    | 0           | 0                         | 100                   | 0           | 0                         |
| Shen multiaxial           | 2             | 80 – 88                | 0           | 12 – 20                   | 72 – 82               | 0           | 18 – 28                   |
| Takahashi uniaxial        | 2             | 100                    | 0           | 0                         | 100                   | 0           | 0                         |
| Takahashi multiaxial      | 2             | 70 – 88                | 0           | 12 – 30                   | 84 – 89               | 0           | 11 – 28                   |
| Takahashi $180^\circ$     | 2             | 59 – 77                | 0           | 23 – 41                   | 61 – 78               | 0           | 22 – 38                   |

## 5 Discussion and outlook

The aim of this paper is to evaluate the EGP criterion and compare the same to the GP criterion. By ignoring the damage caused by  $\sigma_{\parallel}$ , the GP criterion is found to be incapable of correctly assessing multiaxial stress states. A safe and reliable fatigue life calculation is not necessarily given. The reason why the GP criterion only rarely leads to non-conservative results in this paper is that FAT classes with a high survival probability were used. Fatigue tests based on a lower fatigue resistance or a lower survival probability are likely to be evaluated non-conservatively once  $\sigma_{\parallel}$  is applied, especially when the other two stress components tend to be insignificant. In conclusion, the original GP criterion can only correctly assess the fatigue life as long as  $\sigma_{\perp}$  respectively  $\tau$  are dominant.

The EGP criterion correctly and reliably evaluates all stress components by calculating similarly conservative fatigue lives for different multiaxial stress states. The additional damage from  $\sigma_{\parallel}$  obviously only reduces the fatigue life, making all predictions just as safe or safer than those based on the GP criterion. However, specimens subjected to  $\tau$  and evaluated based on notch stresses showed much more conservative results as  $\tau$  increases (see Fig. 7). This indicates that the used FAT classes for  $\tau$  are too conservative and an update may be necessary. As the FAT classes were not specifically derived from the specimens in this paper, some bias in terms of the endurable stresses was always implied. In all other cases, this was unproblematic as the bias was similar for each stress component of a specimen and can therefore be interpreted as a safety factor. Nevertheless, using design S-N curves from codes and standards requires caution.

Whereas the GP criterion is derived from the elliptical relationship between normal and shear stress described in Chapter 2, the EGP criterion assumes that another normal stress component affects fatigue life in the same manner. Although this assumption has proved successful in describing fatigue life, a comprehensive experimental program in which specimens are subjected to each stress component individually and in combination would be beneficial to further confirm this assumption. This way, unbiased results can be obtained as S-N curves with a 50% survival probability can be derived directly from

experiments. Nevertheless, this paper shows how the EGP criterion evaluates fatigue life with significantly higher accuracy and less likelihood of non-conservative results compared to the GP criterion.

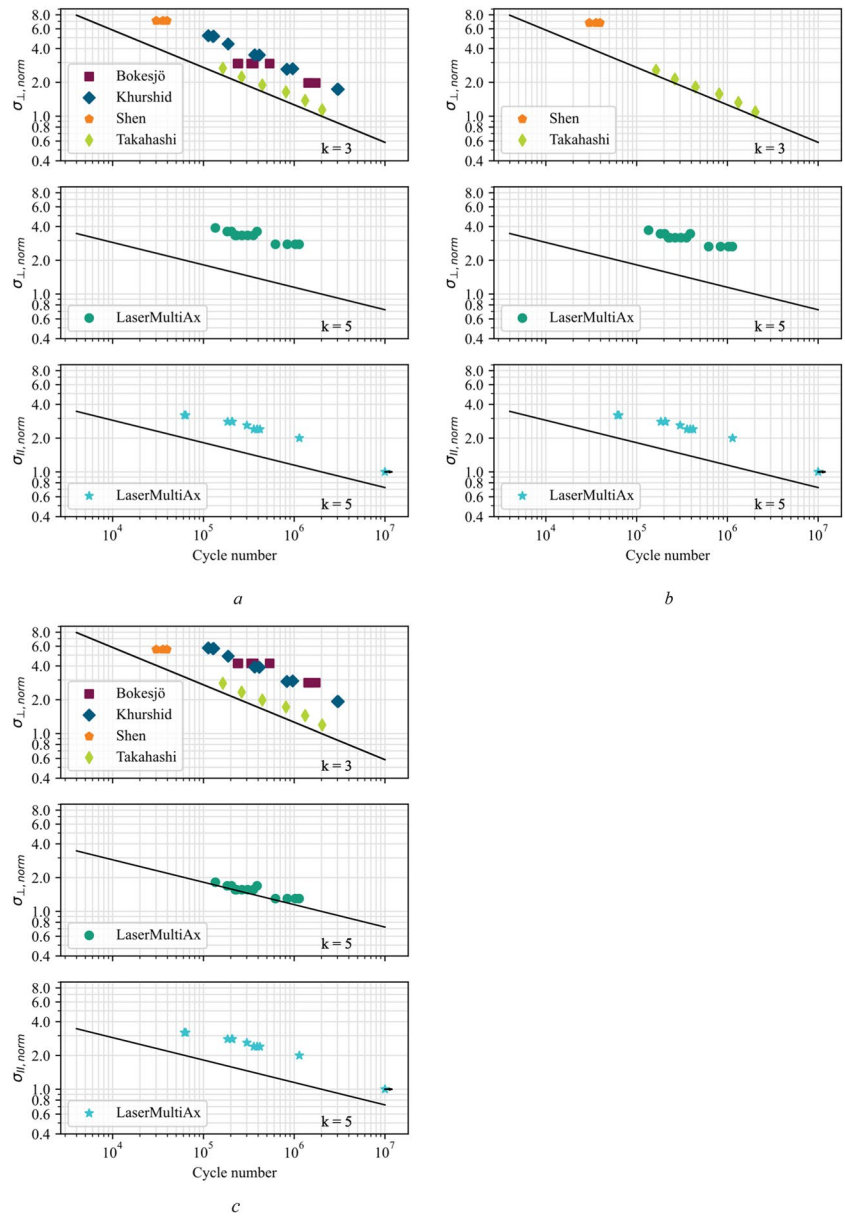
## 6 Conclusion

Evaluating the fatigue life of welded joints subjected to multiaxial stresses usually refers only to stresses normal to the weld and shear stresses. The commonly used Gough-Pollard criterion [1] is found to be unable to correctly assess welded specimens under multiaxial stresses when they include stresses parallel to the weld. Since the Gough-Pollard criterion does not account for damage resulting from this stress component, the calculated fatigue life becomes less conservative as more stress parallel to the weld is applied. The likelihood of non-conservative results is therefore increased. An extension of the Gough-Pollard criterion [6, 7], which additionally considers stresses parallel to the weld, was applied to welded joints for the first time. The extended Gough-Pollard criterion is found to be capable of reliably and conservatively evaluating welded specimens under multiaxial stresses, including all stress components in the plane stress state. Higher accuracy and lower probability of non-conservative results are achieved compared to the Gough-Pollard criterion as all results are similarly conservative. This means that the damage caused by stresses parallel to the weld can be correctly accounted for and deviations in fatigue life calculations between specimens subjected to different stress states can be avoided. The application of the extended Gough-Pollard criterion is therefore always as safe or safer than the original Gough-Pollard criterion and always recommended over the original Gough-Pollard criterion. Both criteria have been applied within the nominal, the hot spot, and the notch stress concept and yield the same results.

In addition, the FAT class for shear stresses and the application of the notch stress approach lead to conservative results. Therefore, an evaluation of fatigue tests with notch stresses should be conducted to verify or update the FAT classes for shear stress.

### Appendix 1. Normalized fatigue data

**Fig. 10** Normalized fatigue data and design S-N curve for uniaxial stress states based on the a. nominal, b. hot spot, and c. notch stress concept



## Appendix 2. Fatigue life evaluation based on the hot spot stress concept

Fig. 11 Numerically evaluated fatigue life over experimental fatigue life based on the hot spot stress concept

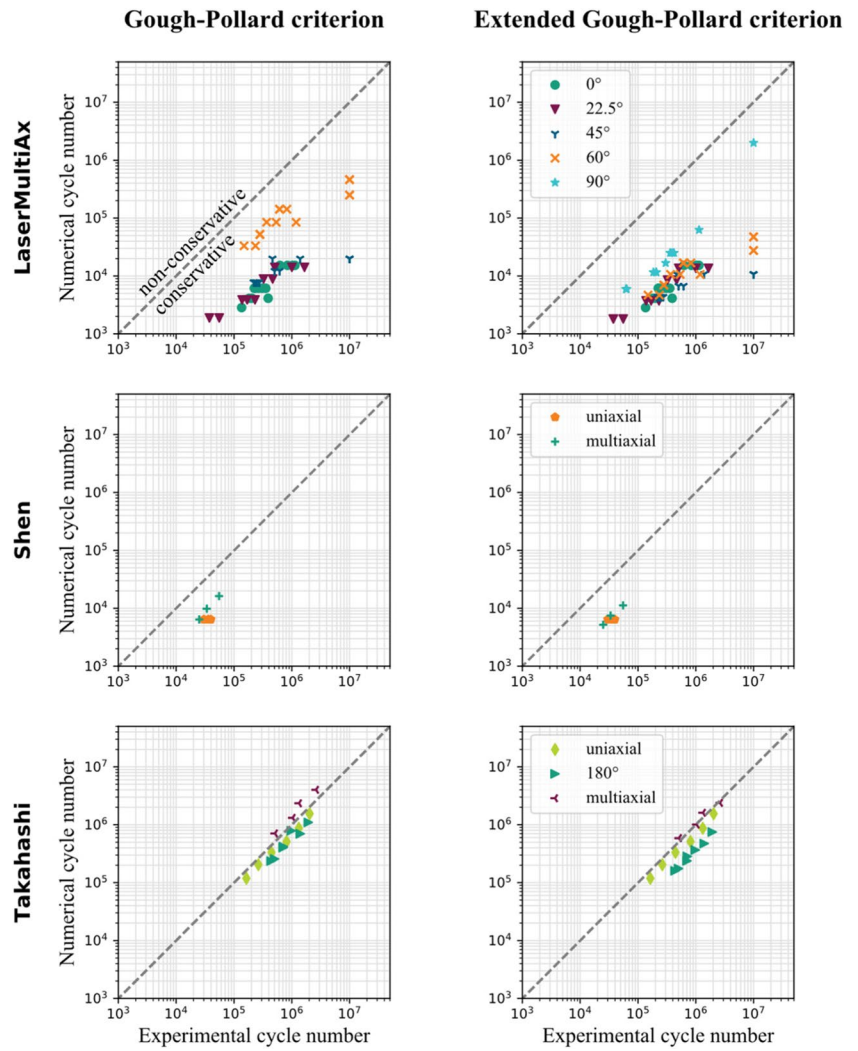
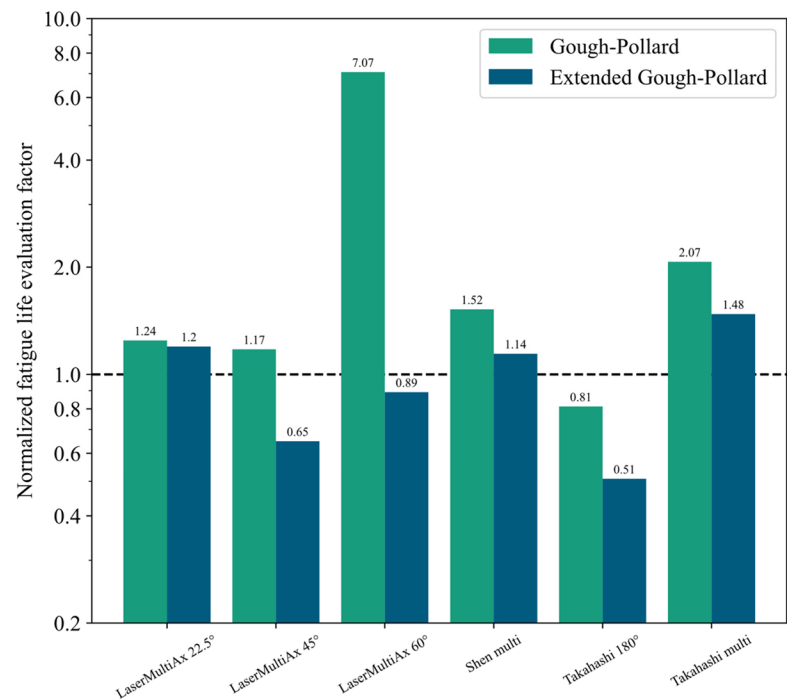


**Fig. 12** Normalized fatigue life evaluation factor for each multi-axial test set based on the hot spot stress concept



**Acknowledgements** The author would like to thank Prof. C. M. Sonsino from the Fraunhofer Institute for Structural Durability and System Reliability LBF for the helpful feedback and discussions and Dr. M. Khurshid from the KTH Royal Institute of Technology for providing further information on the failure types of the fatigue tests.

**Funding** Open Access funding enabled and organized by Projekt DEAL.

## Declarations

**Competing interests** The authors declare no competing interests.

**Open Access** This article is licensed under a Creative Commons Attribution 4.0 International License, which permits use, sharing, adaptation, distribution and reproduction in any medium or format, as long as you give appropriate credit to the original author(s) and the source, provide a link to the Creative Commons licence, and indicate if changes were made. The images or other third party material in this article are included in the article's Creative Commons licence, unless indicated otherwise in a credit line to the material. If material is not included in the article's Creative Commons licence and your intended use is not permitted by statutory regulation or exceeds the permitted use, you will need to obtain permission directly from the copyright holder. To view a copy of this licence, visit <http://creativecommons.org/licenses/by/4.0/>.

## References

- Hobbacher AF (2016) Recommendations for fatigue design of welded joints and components Springer International Publishing. <https://doi.org/10.1007/978-3-319-23757-2>
- Gough HJ, Pollard HV (1935) The strength of metals under combined alternating stresses. Proc Inst Mech Eng 131(1):3–103
- Pedersen MM (2016) Multi-axial fatigue assessment of welded joints using the notch stress approach. Int J Fatigue 83:269–279. <https://doi.org/10.1016/j.ijfatigue.2015.10.021>
- Bokesjö M, Al-Emrani M, Svensson T (2012) Fatigue strength of fillet welds subjected to multi-axial stresses. Int J Fatigue 44:21–31. <https://doi.org/10.1016/j.ijfatigue.2012.06.004>
- Khurshid M, Barsoum Z, Barsoum I et al (2016) The multi-axial weld root fatigue of butt welded joints subjected to uniaxial loading. Fatigue Fract Eng Mater Struct 39(10):1281–1298. <https://doi.org/10.1111/ffe.12444>
- Merkblatt DVS 0905 (2021) Industrielle Anwendung des Kerbspannungskonzeptes für den Ermüdungsfestigkeitsnachweis von Schweißverbindungen (Engl.: Industrial application of the notch stress concept for the fatigue strength assessment of welded joints). DVS – Deutscher Verband für Schweißen und verwandte Verfahren e. V
- Hobbacher AF, Baumgartner J (2023) Recommendations for fatigue design of welded joints and components. Draft Version July 2023
- Sonsino CM (2011) Influence of material's ductility and local deformation mode on multi-axial fatigue response. Int J Fatigue 33(8):930–947. <https://doi.org/10.1016/j.ijfatigue.2011.01.010>
- Shen W, Yan R, Liu E et al (2015) Fatigue growth behavior for surface crack in welding joints under combined compressive and bending stresses. Int J Fatigue 77:50–63. <https://doi.org/10.1016/j.ijfatigue.2015.03.005>
- Takahashi I, Takada A, Ushijima M et al (2003) Fatigue behaviour of a box-welded joint under biaxial cyclic loading: effects of biaxial load range ratio and cyclic compressive loads in the lateral direction. Fatigue Fract Eng Mater Struct 26(5):439–448
- Wagner M, Faß M (2022) Schwingfeste Auslegung laserstrahlgeschweißter Verbindungen unter mehrachsiger Beanspruchung (Engl.: Fatigue resistant design of laser beam welded joints under multi-axial loading). Final report. IGF-Project 20621 BG / 2
- Baumgartner J, Bruder T (2013) An efficient meshing approach for the calculation of notch stresses. Weld World 57:137–145. <https://doi.org/10.1007/s40194-012-0005-3>

**Publisher's Note** Springer Nature remains neutral with regard to jurisdictional claims in published maps and institutional affiliations.